Association of Metallurgical Engineers of Serbia *Scientific paper*
AMES *UDC: 620.193/.196:669.711; 620.197.3*

INFLUENCE OF THE CHEMICAL COMPOSITION ON THE CORROSION PERFORMANCES OF SOME Al-Fe-Si, Al-Mg-Si AND Al-Mg-Mn TYPE ALLOYS

Kemal Delijić[1*], Boštjan Markoli[2], Iztok Naglič[2]

[1]*Faculty of Metallurgy and Technology, University of Montenegro, Cetinjski put, Podgorica, Montenegro,*
[2]*University of Ljubljana, Faculty of Natural Sciences and Engineering, Department of Materials and Metallurgy, Askerčeva 12, Ljubljana, Slovenia*

Received 29.10.2014
Accepted 26.11.2014

Abstract

Paper presents the results on the corrosion behavior of some Al-Fe-Si, Al-Mg-Si and Al-Mg-Mn alloys in their final commercially usable tempered state. Durability of alloys was quantified and compared in the sense of corrosion rates in aqueous solutions while also having in mind the role of alloy chemistry. Open circuit corrosion potential (OCP) measurements, linear polarization and potentiodynamic anodic/cathodic polarization was employed in order to determine the corrosion behavior of samples in the mixture of chloride ions containing aqueous corrosion ambient. We found out that AlFe0.83Si0.18(AA8079), AlMg0.63Si0.72 (AA6005) and AlMg4Mn (AA5182) alloy exhibited the highest rates of passivation in 0.51 mol NaCl solution. The group of Al-Fe-Si alloys exhibited the greatest sensitivity to the changes in chemical composition under potentiodynamic polarization. Artificially aged Al-Mg-Si extruded profiles and fully annealed (after cold rolling) Al-Mg-Mn sheets exhibit very similar levels of equilibrium potentials $E_{(I=0)}$ in 0.51 mol NaCl solution. In the case of Al-Fe-Si alloys, we found that Fe/Si ratio also plays an important role, next to the total content of Fe and Si. Alloys with high Fe/Si ratios showed almost 30 % lower polarization resistance compared to the alloys with balanced Fe/Si, even in the case of the equal total content of alloying elements. The AlMg0.7Si1.2Mn0.8 alloy aged after quenching in the sprayed water and AlMg4Zn1.3Mn0.4 annealed sheet exhibit very similar levels of corrosion rates in 0.51 mol NaCl solution.

Key words: Al-Fe-Si, Al-Mg-Si, Al-Mg-Mn, Sheets, Profiles, Corrosion

[*]Corresponding autor: Kemal Delijić, kemal@ac.me

Introduction

From a corrosion perspective, aluminum and its alloys have been a successful metal materials used for many applications like commodity roles, automotive and vital structural components in aircrafts. There are numerous Al-based alloys successfully used in different environmental or atmospheric conditions either in their conventional form, leaving the corrosion protection industry to focus on market-needs**,** or other more or less demanding applications. Relatively pure aluminum has good corrosion properties due to formation of the strongly bonded barrier oxide film. This protective oxide layer is especially stable in near-neutral solutions of most non-halide salts leading to excellent pitting resistance. Nevertheless, in open-air solutions containing halide ions, with Cl^- ion being the most common, aluminum is susceptible to pitting corrosion [1,2]. This process is related to the presence of oxygen, and the metal is readily polarized to its pitting potential, and because chlorides contribute to the formation of soluble chlorinated aluminum-hydroxide which interferes with the formation of the stable oxide on the aluminum surface [2]. The composition of the aluminum-rich solid solution, which constitutes the predominant volume fraction and area fraction of the microstructure, determines the corrosion potential of an aluminum alloy in a given environment. Alloying elements are added to aluminum for various reasons with improving mechanical properties as the principal reason. These elements introduce heterogeneity into the microstructure, which is the main cause of localized corrosion that initiates in the form of pitting, and each alloying element has a different effect on the corrosion of aluminum [2]. These microstructural heterogeneities frequently have corrosion potentials differing from that of the solid solution matrix resulting in local (micro-) galvanic cells and it which can be experimentally quantified [1, 3-7].

In this paper, we discuss the influence of chemical composition on the corrosion behavior of some Al-Fe-Si, Al-Mg-Si and Al-Mg-Mn alloys in their final commercially usable tempered states. Some of these alloys are used for many automotive applications such as Al-Fe-Si for thin gauge automotive heat exchanger type of applications, Al-Mg-Si alloys for extruded and hydro-formed sections, and Al-Mg-Mn and Al-Mg-Si series alloys for sheet applications, such as inner structural parts and outer skins [8-15].

A substantial portion of Al-Fe-Si and Al-Fe-Mn-Si alloys is also used for manufacturing the packaging foils and sheets for common heat exchanger applications [8, 9]. These Al-rich eutectic alloys based on Al-Fe-Si and Al-Fe-Mn when roll-cast and appropriately processed can provide a good combination of strength and ductility. Their performance depends not only on the mechanical properties but also on the corrosion resistance in working ambient. One of the most important factors being the intermetallic particles, nature of which depends on the chemical composition, dispersed in the aluminum matrix. of foils. Some of these particles may become anodic in most corrosive environments with the respect to the aluminum matrix, micro-galvanic cells may form which lead to the local perforation of the aluminum foil [7, 12, 14, 16, 17]. The growing demand for more fuel-efficient vehicles to reduce energy consumption and air pollution is a challenge for the automotive industry. Highly formable non-heat treatable AA5xxx alloys are used mostly for the inner panel applications, whilst the heat-treatable AA6xxx alloys are preferred for the outer panel applications [19]. The Al-Mg-Mn alloy system gives different combination of superior formability with sufficient strength achieved by the solid solution hardening which can be further enhanced by deformation due to the characteristically high strain hardening behavior. Further

improvement in properties required for specific applications (e.g. surface appearance, corrosion resistance, and thermal stability) has been achieved by small additions of other alloy elements and/or modified processing routes [20-23]. The AA6xxx series of aluminum alloys are very attractive for the application in transportation industry because of their high specific strength to weight ratio and are mostly used where quenching occurs during the extrusion processing. These alloys contain silicon and magnesium approximately in the proportions required to form magnesium-silicide (Mg_2Si) phase. In recent years, alloy modifications have been introduced, together with specific processing modifications, to meet the requirements related to the strength, formability, and paint bake process and corrosion resistance [20]. The rationale behind the development of these alloys and the different performance of the alloys has been covered in many publications, and will not be repeated here.

The objective of this investigation paper was to investigate the corrosion behavior of some Al-F-Si, Al-Mg-Si and Al-Mg-Mn alloys in aqueous solutions, taking into account the role of chemical composition of alloys, by quantifying and comparing the alloy durability in the sense of corrosion rates. Open circuit corrosion potential (OCP) measurements, recorded as a function of time for 60 minutes, linear polarization and the polarization resistance (R_{pol}) measurements, corrosion current (i_{corr}), corrosion rate (Corr rate) and equilibrium potential ($E_{(i=0)}$) were carried out. Additionally, the potentiodynamic anodic and cathodic polarization were employed in order to determine the corrosion behavior of annealed (after cold rolling) Al-Fe-Si Al-Mg-Mn sheets and Al-Mg-Si artificially aged samples.

Experimental Procedure

The chemical composition for the tested series of alloys is given in the Table 1. Thin strips of Al-Fe-Si alloys (AA8xxx) were prepared from twin-roll continuously (TRC) cast strips. Alloys were continuously cast to 7 mm thickness in an industrial "3C" device. Casting speed was 1 m/min and the temperature 690 ^{o}C. Samples of TRC sheets were subsequently industrially cold-rolled to the final thickness of 0.5 mm, with an intermediate annealing (480 ^{o}C for 6 hours) at gauges of 2 mm. The Al-Mg-Si (AA6xxx) alloys used in this experiment were industrially produced from the semi-continuous cast billets and supplied ~~to us~~ in the form of extruded profiles. All tested alloys belong to the AA6xxx series of alloys with the excess of silicon. Cast billets with 7 m in length and a diameter of 0.2 m were homogenized for 12 hours at 570 ^{o}C. They were subsequently cut to the length of 0.62 m and extruded through the hydraulic press with direct metal flow into the rectangular tube, through the single-hole bridge die, with the extrusion ratio of 74. Extruded profiles were quenched directly on the press with the blown air, except for the alloy AlMg0.7Si1.2Mn0.8, which was quenched with the water spray, cooled to room temperature, stretched and subsequently artificially aged under laboratory conditions.

The temperatures of the press container and pre-heated billets were 420 ^{0}C and 520°C, respectively, for all investigated Al-Mg-Si alloys. All specimens were artificially aged at 170 °C for 6 hours after the extrusion. Three Al-Mg-Mn alloys used in the experiment were produced under laboratory conditions. The alloys were cast into steel mold, in the form of plates h×b×l=10×100×200 mm, subsequently homogenized at 470-510 °C (depending on the chemical composition) for 4 hours and cold rolled (with three intermediate annealing) to final thickness of 1.25 mm.

Table 1. Chemical composition of the tested Al-Fe-Si, Al-Mg-Si and Al-Mg alloys (wt. %)

N°	**Commercial designation**	**Type of Alloy**	(Al rest)						
			Mg	**Si**	**Mn**	**Fe**	**Zr**	**Zn**	**Cu**
1	AA8079	AlFe0.83Si0.18		0.18	0.01	0.83			
2	AA1200	AlFe1Si0.18Mn0.14		0.18	0.141	1.04			
3	AA8011	AlFe0.74Si0.52		0.52	0.077	0.74			
4	AA8011	AlFe0.66Si0.58Mn0.37		0.58	0.37	0.66			
5	AA8006	AlFe1.34Si0.14Mn0.43		0.14	0.43	1.34			
6	AA6060	AlMg0.44Si0.54	0.44	0.54	0.006	0.46		0.12	
7	AA6005	AlMg0.63Si0.71	0.63	0.71	0.07	0.23			
8	AA6005*	AlMg0.65Si0.76Zr0.1	0.65	0.76	0.12	0.21	0.1		
9	AA6082	AlMg1Si0.91Mn0.47	1.03	0.92	0.47	0.21			
10	AA6082	AlMg0.7Si1.2Mn0.8	0.7	1.22	0.81	0.23			
11	AA5182	AlMg4Mn0.4	4.23	0.13	0.42	0.26			
12		AlMg4Mn0.4Zn0.3	4.03	0.22	0.43	0.24		0.34	0.16
13		AlMg4Zn1.3Mn0.4	4	0.21	0.21	0.22		1.31	0.18

The samples of Al-Fe-Si and Al-Mg-Mn alloys were tested as recrystallized sheets (fully annealed) after cold rolling, and Al-Mg-Si alloys were tested as heat treated, i.e. artificially aged after quenching. The mechanical properties (tensile strength, yield stress and fracture strain) were determined according to the standard methodology, using the tensile testing "Instron" equipment as presented in the Table 2.

Table 2. Tensile properties of investigated alloys

N°	**Alloy**	**$R_{p0,2}$, MPa**	**R_m, MPa**	**A, %**
N°	AlFe0.83Si0.18	38	91	40
	AlFe1Si0.18Mn0.14	38	97	35
1	AlFe0.74Si0.52	42	112	35
2	AlFe0.66Si0.58Mn0.37	42	117	32
3	AlFe1.34Si0.14Mn0.43	48	127	32
4	AlMg0.44Si0.54	244	266	12
5	AlMg0.63Si0.71	233	272	12
6	AlMg0.65Si0.76Zr0.1	282	311	7
7	AlMg1Si0.91Mn0.47	249	266	11
8	AlMg0.7Si1.2Mn0.8	314	338	14
9	AlMg4Mn0.4	122	252	26
10	AlMg4Mn0.4Zn0.3	142	282	27
11	AlMg4Zn1.3Mn0.4	150	301	29

The PAR-352 system of potentiostat-galvanostat (mod 273), with MK-047 cell and software PAR SOFTCORR 352 II was employed to investigate the corrosion behavior of tested alloys in two aqueous corrosion ambiences: natural water containing 8 mg/dm^{3}of Cl^-, and 0.51 mol sodium chloride solution, as a simulation of seawater conditions. Three different testing techniques listed below, were used in order to evaluate the corrosion behavior of the tested Al-Mg-Si alloys:

1. Open circuit corrosion potential (OCP) measurements, recorded as a function of time for 60 minutes,
2. Linear polarization and measuring the polarization resistance (R_{pol}), corrosion current (i_{corr}), corrosion rate (Corr rate) and equilibrium potential ($E_{(i=0)}$)
3. Potentiodynamic anodic and cathodic polarization, and measurements of the corrosion current (i_{corr}), corrosion rate (Corr rate) and equilibrium potential ($E_{(i=0)}$)

For the purpose of comparison of the corrosion characteristics, the testing of annealed AA1020 (Al99.7) sheet sample was also performed.

Results and Discussion

Corrosion behavior of selected alloys was assessed in natural water and in synthetic seawater, using three accelerated methods of testing. The evolution of corrosion potential for tested alloys, immersed in natural water and in 0.51 mol NaCl solution during one hour, is presented in Figure 1. It can be observed that the onsets of the open circuit corrosion potentials (OCP) for all alloys are shifted in the direction of more electropositive values, and the shapes of the curves that represent the evolution of E_{corr} for different series of tested aluminum alloys are similar. Such a rise in potential in the electropositive direction is usually observed for the samples that exhibit passivity in given corrosion ambience.

The open circuit corrosion potentials of all alloys increase quickly during the first 200 seconds, showing a significant rate of passivation. Comparison of the OCP curves for Al-Fe-Si alloys shows that the highest rate of passivation in 0.51 mol NaCl solution was exhibited by AlFe0.83Si0.18 (AA8079) alloy, Figure 1a. This sample reached a stable value of the open circuit corrosion potential in the first 50 seconds of the immersion. In the cases of Al-Mg-Si (Figure 1b) and Al-Mg-Mn (Figure 1c) alloys, the highest rates of passivation are indicated for AlMg0.63Si0.72 and AlMg4Mn alloys, respectively.

Final values of the corrosion potential, after 60 minutes, its dependence on the type of alloy and, in general, on the total alloying elements content, are all illustrated in Figure 2. Final open circuit corrosion potentials of all alloys were in the ranges between -579mV and -759 mV in natural water, and between -730 mV and -894 mV in 0.51 mol NaCl solution.

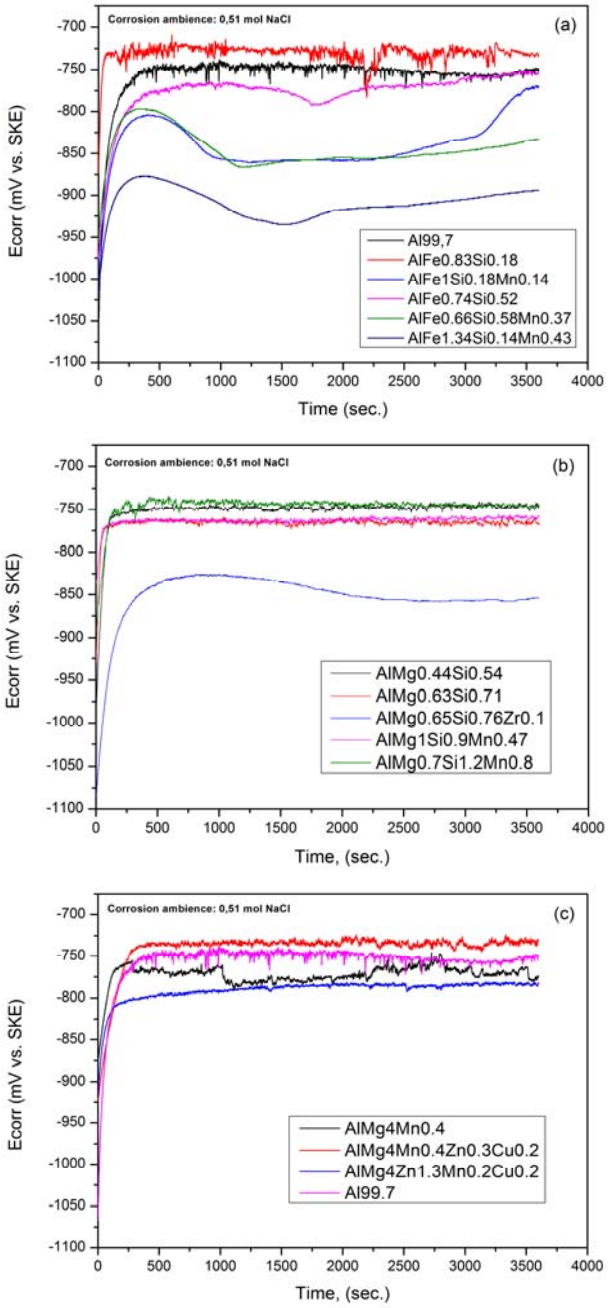

Fig. 1. Open circuit potential vs. time of tested (a) Al-Fe-Si, (b) Al-Mg-Si and (c) Al-Mg-Mn alloys in synthetic seawater, open to air at room temperature.

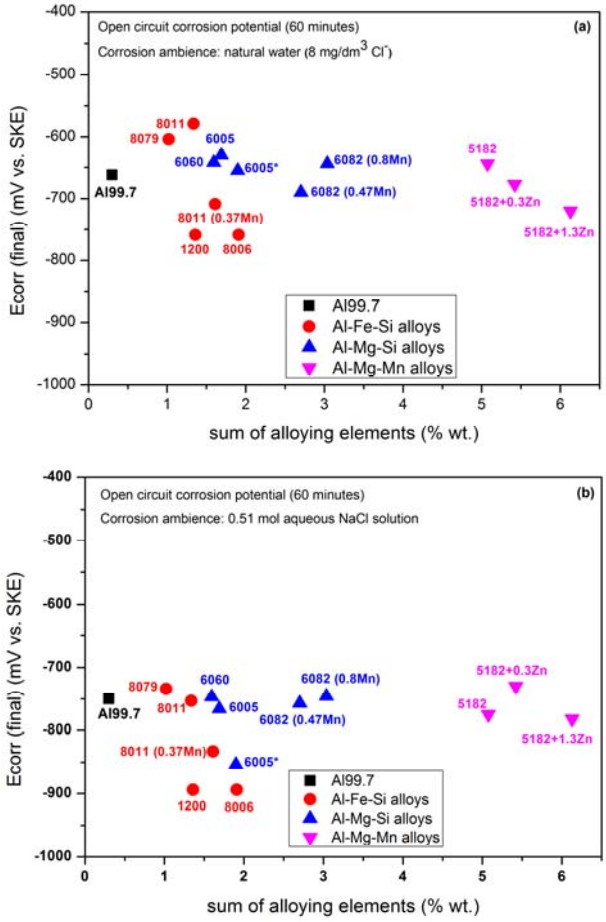

Fig. 2. Effect of the total alloying elements content on the final values of OCPs of tested Al-Fe-Si, Al-Mg-Si and Al-Mg-Mn alloys in (a) natural water and (b) synthetic seawater, open to air at room temperature

Open circuit corrosion potentials of cold-rolled and annealed Al-Fe-Si thin sheets, with high Fe/Si ratios, or containing higher percentage of Fe and Mn (AlFe1Si0.18Mn0.14, AlFe1.34Si0.14Mn0.43, AlFe0.66Si0.58Mn0.37), are shifted towards more electronegative values, if compared to the Al99.7 values in both corrosion ambient. Differences in the values of the OCPs for the Al-Fe-Si samples and Al99.7 were about 14% (approx. 100 mV) in natural water and 19% (approx. 140 mV) in seawater. The OCPs of tested AA5xxx and AA6xxx alloys were quite close and comparable with the OCPs of annealed Al99.7 sheet sample, in both corrosion ambient. Differences in OCPs of these alloys, in relation to Al99.7, were between 1-4 %. The exceptions were found for the AlMg0.65Si0.76Zr0.1 alloy in chloride solution where the difference is 14 % (about 100 mV) and for the AlMg4Zn1.3Mn0.4 sample immersed in natural water (about 9%, or 60mV) [24].

Figure 3 shows polarization curves of investigated alloys under potentiodynamic scanning conditions in synthetic seawater.

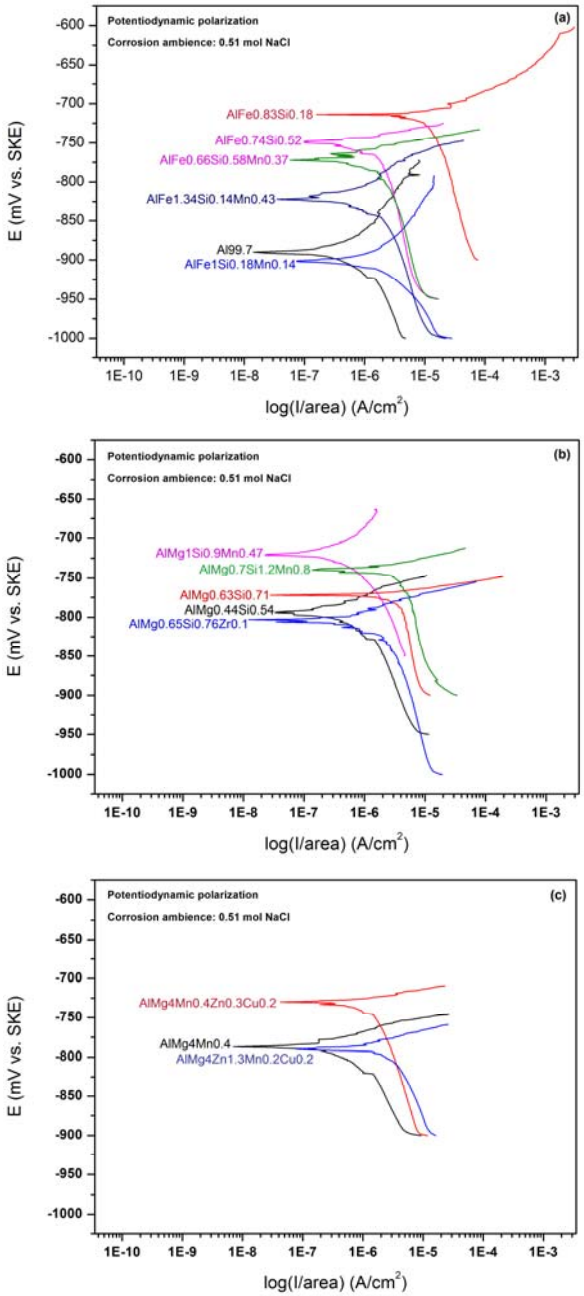

Fig. 3.Potentiodynamic polarization diagrams of tested (a) Al-Fe-Si, (b) Al-Mg-Si and (c) Al-Mg alloys samples in synthetic seawater, open to air at room temperature

Similarities in the shapes of the anodic and cathodic parts of the potentiodynamic scanning curves, but also some differences in the slopes of anodic parts, which promote dissolution and corresponds to the corrosion rates illustrated in Figure 4b, are evident for all group of samples. Some of the corresponding calculated corrosion parameters (the equilibrium potential and corrosion current) are presented in Figure 4. It is clear that the Al-Fe-Si group of tested alloys exhibited the greatest sensitivity to the changes in the content of alloying elements under potentiodynamic polarization. The increase in the total content of Fe, Si and Mn for 1wt. % moved potentiodynamic curves to more electronegative values of potential by about 200 mV. Artificially aged Al-Mg-Si extruded profiles and fully annealed (after cold rolling) Al-Mg-Mn sheets exhibit very similar levels of equilibrium potentials $E_{(I=0)}$in 0.51 mol NaCl solution, Figure 4a. The increase in the total content of main alloying elements in tested Al-Mg-Si alloys slightly moved the equilibrium potentials $E_{(I=0)}$ to the "more noble" areas of less negative potentials.

Values of the equilibrium potentials $E_{(I=0)}$for the reactions under consideration of potentiodynamic scanning conditions (anodic or cathodic) of all tested alloys, in 0.51 mol NaCl solution, were in the following ranges (Figure 4a):

- between -714 mV and -901 mV for Al-Fe-Si alloys,
- between -739 mV and -805 mV for Al-Mg-Si alloys,
- between -729 mV and -789 mV for Al-Mg-Mn alloys.

Figure 4b illustrates the values of corrosion current as a function of the type of alloy for potentiodynamic conditions of testing in synthetic seawater, open to air at room temperature. Corrosion currents generally increase with increasing content of alloying elements inside of all groups of alloys. The increase in corrosion current density was most pronounced in the Al-Mg-Si alloys: increase in the content of the main alloying elements to about 1.5wt.% caused an increase in i_{corr} for three to five times compared toAl99.7 or to basic AlMg0.44Si0.54 alloy. It is well known that the addition of Si in conjunction with Mg, which is typical in AA6xxx series of Al alloys, allows Mg_2Si particles to precipitate. There is also a lot of literature data on the role of chemical composition on forming the Mg-Si phase and its influence on mechanical properties [2, 25-27]. These particles are beneficial in terms of increasing strength, but as shown in recent investigations, that Mg_2Si remained more ‘anodic’ than the matrix in Al-alloys. Consequently, Mg_2Si remains anodic and undergoes selective dissolution in the Al-matrix. In a similar way, the results of monitoring of corrosion current of the Al-Mg sheets in 0.51 mol NaCl showed that i_{corr} increases with the addition of Zn and Cu in basic AA5182 alloy.

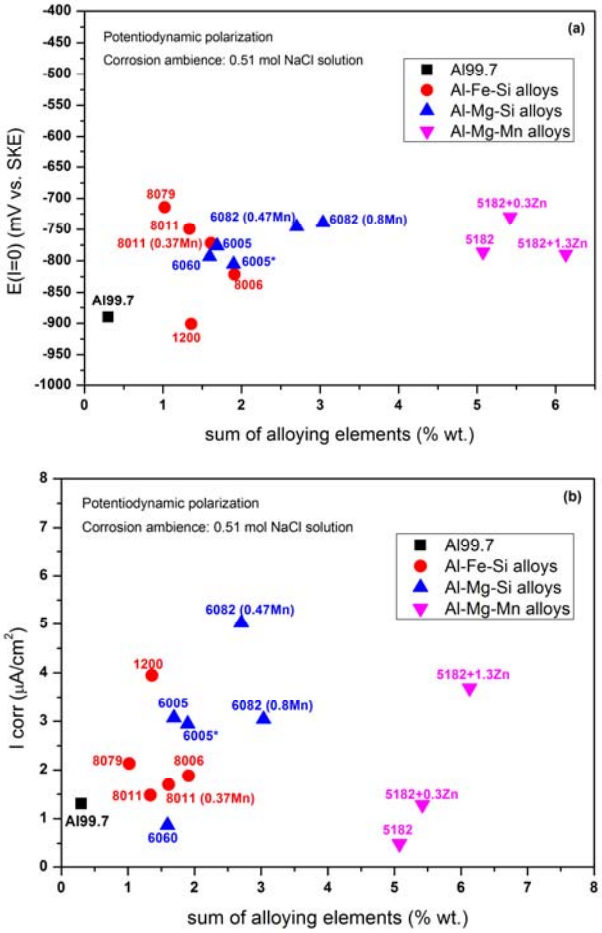

Fig. 4. Effect of the total alloying elements content on the (a) equilibrium potentials and (b) corrosion current of tested Al-Fe-Si, Al-Mg-Si and Al-Mg-Mn alloys samples in synthetic seawater, open to air at room temperature under potentiodynamic polarization conditions

The influence of the chemical composition on the polarization resistance and corrosion current of tested Al-Fe-Si, Al-Mg-Si and Al-Mg-Mn alloys under linear polarization in natural water and synthetic sea water, open to air at room temperature, is illustrated in Figures 5-7. The polarization resistance rapidly decreased with the increasing of the main alloying elements content for all types of alloys. In the case of Al-Fe-Si alloys, it was observed that the Fe/Si ratio also played an important role next to the total content of Fe and Si.

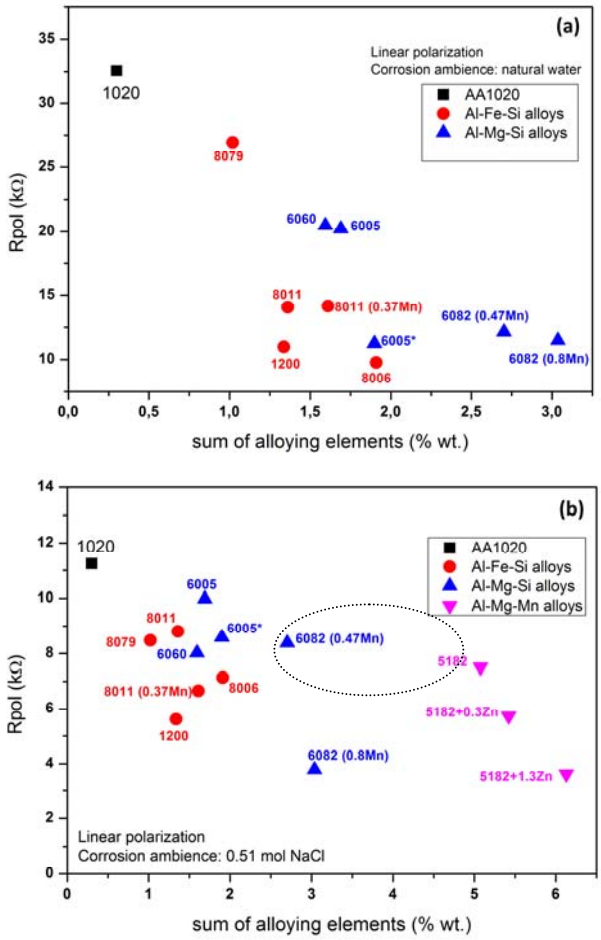

Fig. 5. Effect of the total alloying elements content on the polarization resistance of tested Al-Fe-Si, Al-Mg-Si and Al-Mg-Mn alloys samples under linear polarization (a) natural water and (b) synthetic seawater, open to air at room temperature

Alloys with balanced Fe/Si ratio (AA8011) show significantly higher polarization resistance when compared to alloys with excess of Fe relative to Si (AA1200, AA8006) in natural water even in the case of the equal total content of alloying elements. Results of the linear polarization of Al-Mg-Si alloys indicate that alloys AlMg0.44Si0.54 and AlMg0.63Si0.71 show similar values of polarization resistance, corrosion current and, subsequently, the corrosion rates in natural water. Increasing the Mg+Si+Mn content by1.5 wt.% in this type of alloy decreased the R_{pol} by about 10kΩ. Similar relations between investigated corrosion characteristics for all series of alloys were observed in solution with an elevated concentration of Cl^- ions, Figure 5b. Al-Fe-Si alloys with high Fe/Si ratios and the addition of Mn show about 30% lower values of R_{pol} compared to the alloys with balanced Fe/Si. Al-Mg-Si series of alloys in these testing conditions showed less sensitivity, with the grouping of the

values of the R_{pol} and corrosion currents for samples artificially aged after quenching in blown air. The AlMg0.7Si1.2Mn0.8 alloy aged after quenching in the sprayed water showed significantly lower polarization resistance compared to similar alloys exposed to the effects of slower quenching. Investigated Al-Mg-Mn alloys showed significant corrosion sensitivity with addition of Zn and Cu in aqueous solution with high content of Cl^- ions.

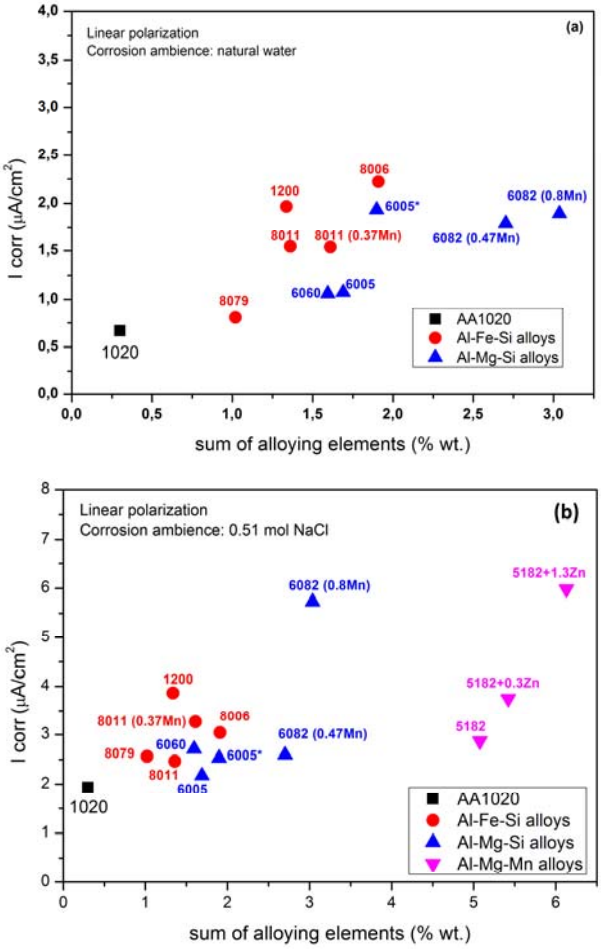

Fig. 6. Effect of the total alloying elements content on the corrosion current under linear polarization (a) natural water and (b) synthetic seawater, open to air at room temperature.

It was found that the addition of 1.3 wt.% Zn and 0.17wt.% Cu to 5182 base alloy, containing 4 wt.% Mg, resulted in significant decrease of R_{pol} (from 7.5kΩ to 3.6 kΩ) and increase of the corrosion current/rates of these annealed sheets for almost two times. It should be noted that base AA5182 alloy showed similar levels of measured corrosion properties in terms of R_{pol} and I_{corr} as AlFe1.34Si0.14Mn0.43 alloy. In addition, AlMg0.7Si1.2Mn0.8 alloy aged after quenching in the sprayed water and

AlMg4Zn1.3Mn0.4 annealed sheet exhibit very similar levels of corrosion current and subsequently corrosion rates in 0.51 mol NaCl solution.

The influence of the chemical composition on the equilibrium potentials ($E_{I=0}$) of tested Al-Fe-Si, Al-Mg-Si and Al-Mg-Mn alloys under linear polarization is presented in Figure 7. The increase of the Fe, Si and Mn content in Al-Fe-Si annealed sheets moved the equilibrium potentials ($E_{I=0}$) in the direction of more electronegative values in natural water, and measured differences were about 225mV. Equilibrium potentials measured on Al-Mg-Si artificially aged samples in natural water are quite close to the values measured on the Al-Fe-Si annealed samples.

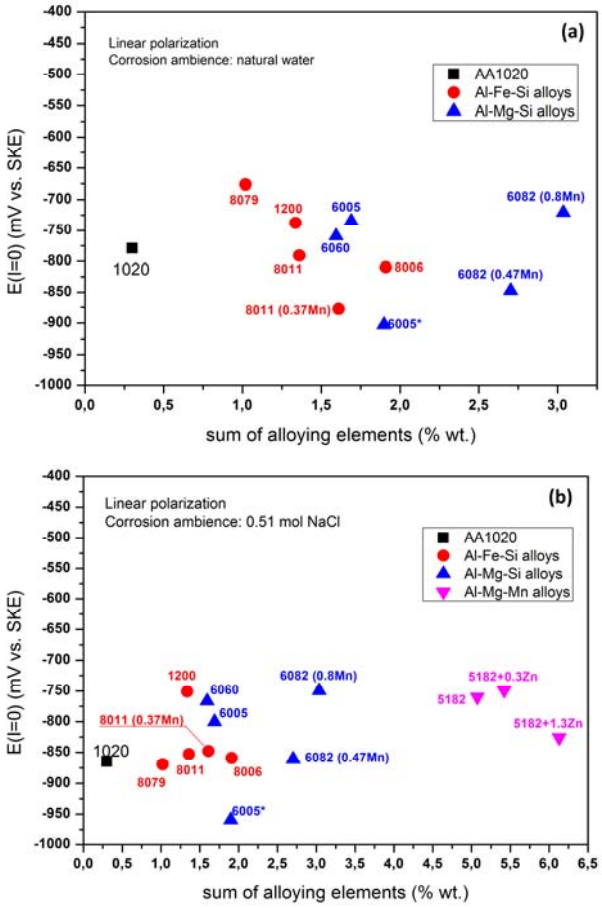

Fig. 7. Effect of the total alloying elements content on the equilibrium potentials of tested Al-Fe-Si, Al-Mg-Si and Al-Mg-Mn alloys samples under linear polarization (a) natural water and (b) synthetic seawater, open to air at room temperature.

Analysis of the correlation between corrosion rates of alloys investigated in 0.51 mol NaCl and their tensile strengths is illustrated in Figure 8. The increase in the strength of certain types of alloys is, generally, a direct consequence of the increase in

the content of alloying elements. In this regard, there is a direct correlation between the increase in the strength of these alloys, and accordingly, the increase in corrosion rate or the reduction of its corrosion resistance. In the case of Al-Mg-Mn alloys, in which the additional alloying of base AA5182 alloy with 1.3 wt.% Zn and 0.18 wt.% Cu increases R_m by about 20%, reaching 300MPa, increased corrosion rate, exponentially, almost twice the initial value. It is worthwhile noting, that in fact this is a very thin layer with formation of about 2.5 µm per year.

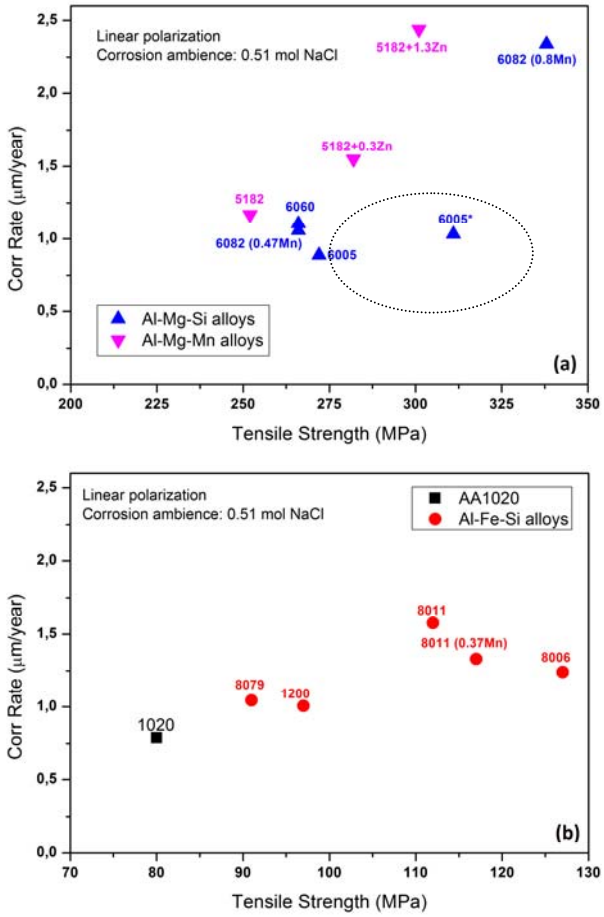

Fig. 8. Corrosion rates in synthetic seawater of tested (a) Al-Mg-Si, Al-Mg-Mn, and (b) Al-Fe-Si alloys under linear polarization against tensile strength, open to air at room temperature.

Very similar corrosion rates were observed by comparing certain Al-Mg-Si and Al-Mg-Mn alloys, which are very close in tensile strength. Thus, same levels of corrosion rates were observed for the non-heat treatable annealed AlMg4Zn1.3Mn0.4 and heat-treatable AlMg0.7Si1.2Mn0.8 alloy aged after quenching in the sprayed water, noting that both alloys exhibit the tensile strength above 300 MPa, Figure 8a, Table 2.

The resulting corrosion parameters for the Al-Fe-Si thin strip in the annealed condition, in terms of correlation and with respect to the tensile strength, indicate relation that may be characterized as a linear interdependence, Figure 8b.

Conclusion

The influence of chemical composition on the corrosion behavior and some correlative interdependence between corrosion durability with tensile strength of Al-Fe-Si, Al-Mg-Si and Al-Mg-Mn type of alloys were investigated. The samples of Al-Fe-Si and Al-Mg-Mn alloys were tested as recrystallized sheets (fully annealed) after cold rolling, and whereas Al-Mg-Si alloys were tested as heat treated - artificially aged after quenching directly on the extrusion press.

The onsets of the open circuit corrosion potentials (OCP) for all group of alloys were shifted in the direction of more electropositive values, and the shapes of the curves that represent the evolution of E_{corr} for different series of tested group of aluminum alloys are similar. The open circuit corrosion potentials of all alloys increase quickly during the first 200 seconds, showing a significant rate of passivation. The highest rates of passivation in 0.51 mol NaCl solution exhibited AlFe0.83Si0.18 (AA8079), AlMg0.63Si0.72 (AA6005) and AlMg4Mn (AA5182) alloys. Increasing the amount of alloying elements in all tested series of alloys shifted the final values of OCPs to less "noble" potential values. It was found that OCPs of tested AA5xxx and AA6xxx alloys are close to the OCPs of annealed Al99.7 sheet sample, in both corrosion ambiences.

The greatest sensitivity to the changes in chemical composition, under potentiodynamic polarization, exhibited the group of Al-Fe-Si alloys. The increase in the total amount of Fe, Si and Mn for 1wt.% moved potentiodynamic curves to more electronegative values of potential by about 200 mV. Artificially aged Al-Mg-Si extruded profiles and fully annealed (after cold rolling) Al-Mg-Mn sheets exhibit very similar levels of equilibrium potentials $E_{(I=0)}$in 0.51 mol NaCl solution. The increase in corrosion current density is most pronounced in the Al-Mg-Si alloys: increase in the content of the main alloying elements to about 1.5 wt.% caused an increase in i_{corr} for three to five times compared toAl99.7or basic AlMg0.44Si0.54 alloy.

The polarization resistance rapidly decreased with the increasing of alloying elements content for all types of alloys. It was observed that in the case of Al-Fe-Si alloys Fe/Si ratio plays an important role also next to the total content of Fe and Si. That is, alloys with high Fe/Si ratios and the addition of Mn showed lower polarization resistance compared to the alloys with balanced Fe/Si, even in the case of the equal total content of alloying elements. Increasing the content of Mg+Si+Mn in Al-Mg-Si type of alloys for 1.5 wt.% decreased the R_{pol} for about 10kΩ. Addition of 1.3 wt.% of Zn and 0.17 wt. % of Cu to base AA5182 alloy, containing 4 wt. % of Mg, resulted in significant decrease of R_{pol} (from 7.5kΩ to 3.6 kΩ) and increase of the corrosion current/rates of these annealed sheets for almost two times. It should be noted that base AA5182 alloy showed similar levels of measured corrosion properties in terms of R_{pol} and i_{corr} as for the AlFe1.34Si0.14Mn0.43 alloy. In addition, AlMg0.7Si1.2Mn0.8 alloy aged after quenching in the sprayed water and AlMg4Zn1.3Mn0.4 annealed sheet exhibit very similar levels of corrosion current and subsequently corrosion rates in 0.51 mol NaCl solution.

References

[1] J. R. Davis, Corrosion of Aluminum and Aluminum Alloys, Materials Park,OH: ASM International, 1999.
[2] N. L. Sukiman, X. Zhou, N. Birbilis, A.E. Hughes, J. M. C. Mol, S. J. Garcia, X. Zhou and G. E. Thompson (2012). Durability and Corrosion of Aluminium and Its Alloys: Overview, Property Space, Techniques and Developments, Aluminium Alloys - New Trends in Fabrication and Applications, Prof. Zaki Ahmad (Ed.), InTech, DOI: 10.5772/53752
[3] V.Guillaumin and G. Mankowski, Corros. Sci. 41(3) (1998) 421-438.
[4] V.Guillaumin and G. Mankowsk,i Corros. Sci. 42(1) (2000) 105-125.
[5] W.Zhang and G. S. Frankel, Electrochim. Acta 48(9) (2003) 1193-1210.
[6] N.Birbilisand R. G. Buchheit, J. Electrochem. Soc. 152(4) (2005) B140.
[7] N.Birbilis, T. Muster, Et Al. Corrosion of Aluminum Alloys. Corrosion Mechanisms in Theory and Practice, Third Edition, CRC Press: 705-736,(2011).
[8] Y.Birol, Homogenization of Twin Roll Cast Al-Fe-Si Alloy Strips, 10th Int. Met. and Mat. Congress, Istanbul Proc. 2000, 1005-1011.
[9] J. Strid, Proc. 3rd Int. Conf. On Aluminum Alloys, The Norwegian Inst. Of Technol. 1992, Vol 3.321.
[10] M.Slamova et al., Proc. 6th Int. Conf. On Aluminum Alloys, Toyohashi, Japan, 1998, Vol. 1., 1287.
[11] A.Kawahara et al., Furukawa Review 24 (2008) 81-87.
[12] R.Mahmudi, M. Aghaie-Khafri Forming Behavior of Roll-Cast Aa8079 Aluminum Alloy Sheet, Aluminum 74(10) (1998) 753-758.
[13] Aluminum and Aluminum Alloys, ASM International, Ohio P 579, 1993.
[14] M. Gupta, D. Cook, J Sahai, Strip Casting Of Aluminum Using Twin Roll Casters, Light Metals 1999, TMS 925.
[15] D.J. Lloyd, Some Aspects Of The Metallurgy Of Automotive Al Alloys, Institute Of Materials Engineering Australasia Ltd., Materials Forum, 28, 2004, 107-117.
[16] M.Slamova, M.Karlik, M.Cieslar, B.Chalupa, P.Merle, Kovove Mater., 41(C.1) (2003) 51-62.
[17] M.Slamova, M.Karlik, M.Cieslar, B.Chalupa, P.Merle, Kovove Mater, 40(C.6) (2002) 389-401.
[18] Y.Birol, F.Birol, Corrosion Behavior Of Twin Roll Cast Al-Mg And Al-Mg-Si Alloys, Institute Of Materials Engineering Australasia Ltd, Materials Forum, 28, 2004, 338-344.
[19] W.S. Miller, L. Zhuang, J. Bottema, A.J. Wittebrood, P. De Smet, A. Haszler, A. Vieregge, Mater. Sci. Eng. A280 (2000) 37–49.
[20] J. Hirsch, Automotive Trends in Aluminium - The European Perspective, Institute Of Materials Engineering Australasia Ltd, Materials Forum, 28, 2004, 15-23.
[21] E.Romhanji, M.Popovic, Metalurgija-Journal of Metallurgy 12(4) (2006) 297-308.
[22] E. Romhanji, M. Popovic, D. Glisic, R. Dodok, D. Jovanovic, Metalurgija-Journal of Metallurgy 11(4) (2005) 267-272.
[23] T.Haga, M.Mtsuo et al., Journal of Achievements in Materials and manufacturing Engineering 34(2) (2009) 172-179.
[24] K. Delijić, B. Markoli, Metallurgical&Materials Engineering 20(2) (2014) 131-140.
[25] S. M.Hirth, G. J. Marshall et al., Materials Science and Engineering A 319-321: 452-456,(2001).

[26] M.Usta, M. E. Glicksman, et al., Mater. Sci. Eng. A35(2) (2004) 435-438.
[27] F.-l.Zeng, Z.-l. Wei, et al., Transactions of Nonferrous Metals Society of China 21(12) (2011) 2559-2567.